12TH INTERNATIONAL SYMPOSIUM ON FLOW VISUALIZATION
September 10-14, 2006, German Aerospace Center (DLR), Göttingen, Germany

HIGH SPEED VISUALIZATION OF FLAME RESPONSE IN A LOX/H2 COMBUSTION CHAMBER DURING EXTERNAL EXCITATION

Bernhard Knapp, Michael Oschwald
Deutsches Zentrum für Luft- und Raumfahrt e.V., Langer Grund, D-74239 Hardthausen

ABSTRACT

With a model combustion chamber the interaction of an acoustic excitation with a burning LOX/H2 spray was investigated. Pressure oscillations are coupled into the combustion chamber by an additional exhaust nozzle and a siren wheel. Due to the fact that the orientation of the excited acoustic modes can be fixed with this secondary nozzle it is possible to investigate the interaction of acoustics with combustion chamber processes like injection, atomization, vaporization, mixture formation and combustion either with the spray in a pressure node or anti node. Thus the role of pressure or velocity coupling with the processes mentioned above can be studied. For a variety of injection conditions the interaction of the acoustic excitation with the spray flame has been investigated. Only damped acoustic oscillations have been observed, at no operating conditions combustion instabilities were found. High speed visualization of the OH emission of the flame is used to get information on the spatially and temporally resolved evolution of the heat release. From the OH-emission and dynamic pressure recordings a response factor of the combustion process is determined for the case of the excitation of the first tangential mode (1T). The acoustic 1T-resonances of the combustor show non-Lorentzian line profiles. There is indication that the excited modes are not pure but that there is always a superposition of various different eigenmodes in the combustion chamber. This complex dynamics of the acoustic field is not well understood up to now.

1 INTRODUCTION

Combustion instabilities still rank among the most difficult problems during the development of (rocket) combustion chambers. During an instability the heat release is modulated by an acoustic field, a feedback loop occurs and the system is potentially unstable. Above all the accompanying increase of the heat transfer to the combustion chamber wall leads to a serious endangering potential and the risk of losing the complete mission.

The main problem now lies in understanding the mechanisms, by which an acoustic oscillation controls the local heat release rate. Heat release in a combustion chamber is the result of a complex succession of processes (injection, atomization, vaporization, mixture and combustion). All can be influenced in any way by an acoustic disturbance. Basically there are two kinds of interaction with an acoustic wave: First the influence by acoustic pressure coupling and second by acoustic velocity coupling. Since many years these coupling mechanisms were investigated intensively [1, 2]. Despite tremendous efforts it was not successful up to now to identify the basic interactions between acoustics and the combustion chamber processes. That's why at DLR, Space Propulsion Institute Lampoldshausen, basic investigations are carried out with a special research combustion chamber.

2 FUNDAMENTALS

2.1 Rayleigh Criterion and Response-Factor

As soon as an acoustic field modulates the heat release in a system a feedback loop occurs and the system is potentially unstable. At the end of the 18th century J.W.S. Rayleigh already has found out that at the moment of the highest compression of a gas heat must be periodically supplied to excite an acoustic instability. This association is well known as Rayleigh criterion. His prediction is based on the phase shift between heat release and pressure oscillation. The mathematical formulation of this criterion is seen by Putnam [3] as necessary but not as a sufficient condition and has the form

$$\iiint \int_0^{2\pi} p'q'dt\,dV > 0 , \tag{1}$$

where p' and q' are the fluctuations of pressure p and heat release q. This condition describes only the energy supply by the combustion to an acoustic system. A self excited acoustic instability can only appear if the phase between q' of an acoustic field and p' is less than $\pm 90°$. In this case the Rayleigh criterion is positive. If this criterion is negative energy supply by the combustion process is damping the acoustic oscillation. The stability of combustion depends on two factors: first the phase shift between the fluctuations of heat release and pressure oscillations and second the damping by the combustion chamber. Heidmann and Wieber [4] defined the following response factor

$$N = \frac{\int_V \int_0^{2\pi} p'(V,t)\cdot q'(V,t)\,dt\,dV}{\int_V \int_0^{2\pi} [p'(V,t)]^2\,dt\,dV} . \tag{2}$$

This factor is based on the Rayleigh criterion and defines a normalized value that evaluates the scale of amplification of the acoustics due to combustion. Assuming that the relative fluctuations p' and q' show a harmonic temporal dependency and heat release $q'(t)=q'_{max}\cdot\sin(\omega t+\varphi)$ is shifted by the phase φ compared with the pressure $p'(t)=p'_{max}\cdot\sin(\omega t)$ the response factor is $N=q'_{max}/p'_{max}\cdot\cos\varphi$.

The determination of N requires knowledge of the heat release. In the reaction front of a H2/O2 flame the OH-radical is produced in an excited electronic state. The intensity I of the chemi-luminescence of these radicals is taken as a measure for the heat release. The amplitude I'_{max} of the variation of the OH-intensity I around the mean $\bar{I}$, i.e. $I=\bar{I}+I'_{max}\cdot\cos(\omega t+\varphi)$, is identified with the heat release fluctuation due to the coupling of the acoustics to the combustion process. The heat release fluctuation q' is substituted with the relative fluctuation of the intensity I'_{max}. By simultaneous measurement of dynamic pressure and OH flame emission this response factor can be determined:

$$N = \frac{I'_{max}}{p'_{max}}\cdot\cos\varphi . \tag{3}$$

2.2 Pressure and Velocity Coupling

There are two basic kinds of interaction processes of acoustics with combustion. The acoustic field can couple to combustion by pressure sensitive processes, like chemical reactions rates, injection rates, and evaporation rates. On the other hand there are coupling processes which are sensitive to the velocity of the acoustic field, like atomization, mixing, and evaporation.

The main question is which of both mechanisms mentioned above dominates in rocket combustion chambers during acoustic instabilities. It has also to be taken in consideration that in different propulsion systems also different coupling mechanisms can be appear.

2.3 Acoustics of a Cylindrical Volume and Orientation of Modes

In linear acoustics the eigenvalue problem $\Delta p' + \alpha \cdot p' = 0$ for a cylindrical resonator can be solved analytically and the pressure distribution in cylindrical coordinates can be calculated as follows

$$p'(r,\varphi,z,t) = \sin(\omega t)\cos\left(l\pi\frac{z}{L}\right)\cos(n\varphi)J_n\left(\alpha_{nm}\frac{r}{R}\right). \tag{4}$$

The coefficients l, n and α_{nm} determine the symmetry of the corresponding modes in the three coordinates r, φ and z. Because of the rotational symmetry of the combustion chamber two solutions of the tangential modes for the same eigenvalue are existing. That means that the orientation of the tangential modes at one eigenfrequency can appear in two shapes and no explicit boundary condition can be given. So a further possible orientation of the 1T mode is rotated 90°, at the 2T mode it is rotated 45° etc. The frequency f_{mn} of the transverse modes is [2]:

$$f_{nm} = \frac{\alpha_{nm}c}{2\pi R}. \tag{5}$$

In the consideration above it was assumed that only the combustion chamber acts as a resonator. The installation of an additional nozzle to excite the combustion chamber acoustically changes the resonance volume in so far as this secondary nozzle acts as an additional resonator which is coupled to the combustion chamber. This additional resonator changes strongly the resonance conditions of the eigenvalue problem. A simple analytical solution is not longer possible, the solution of the wave equation for this problem can only be found numerically.

The breaking of the rotational symmetry by mounting a secondary nozzle leads to non-degenerate tangential modes. The original degenerate tangential modes are split into two separate orientations of the modes with different eigenvalues. The two components of the tangential modes are called as σ- or π-modes (see Fig. 1).
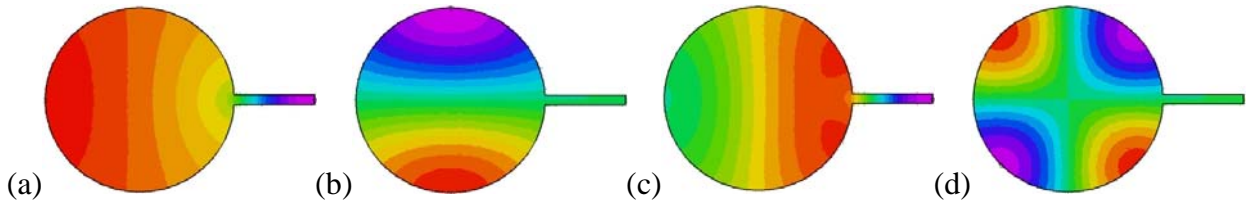

(a)　　　　　(b)　　　　　(c)　　　　　(d)

Fig. 1: Eigenmodes of a cylindrical resonator with cavity: (a) 1Tσ mode, (b), 1Tπ mode, (c) 2Tσ mode, (d) 2Tπ mode

3 EXPERIMENTAL SETUP, TEST PERFORMANCE AND DATA ANALYSIS

The test bench is equipped with a supply system for the cryogenic propellant combination liquid oxygen (LOX) and gaseous hydrogen (GH2) as well as further supply gases like nitrogen and helium. Propellant run-tanks and feed lines are submerged in a tank filled with liquid nitrogen (LN2) at $77K$. Before a test gaseous oxygen is filled in the run-tank and due to the low temperature oxygen is liquefied.

3.1 Combustion Chamber and External Excitation

The combustion chamber is equivalent to a cylindrical resonator with a length five times smaller than the diameter. This geometry was chosen to shift the longitudinal modes to higher frequencies and to minimize their influence to the transverse modes.

An extremely high degree of flexibility during the investigations is guaranteed by 16 evenly distributed modules at the circumference of the combustion chamber. These modules can be equipped with different sensors like dynamic and static pressure sensors or temperature sensors.
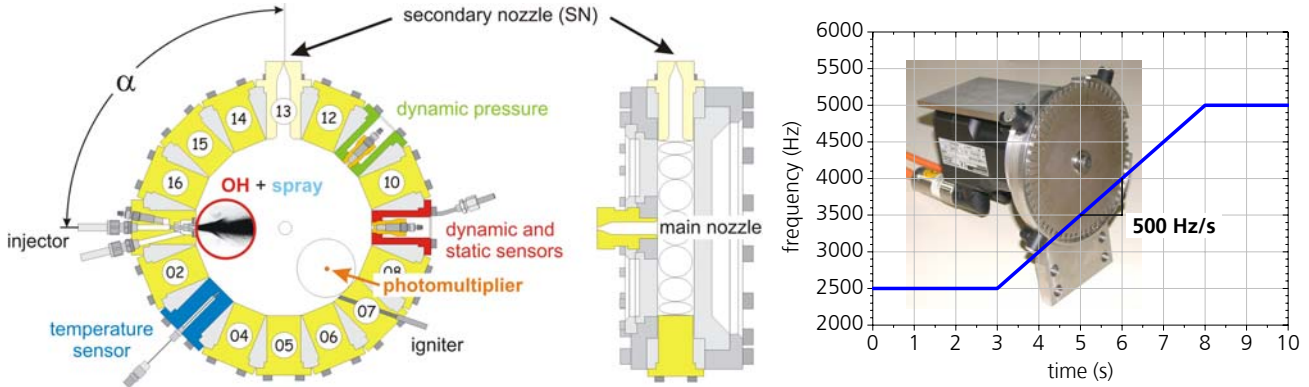
Fig. 2: Left side: Combustion chamber. Right side: siren for external excitation and linear frequency ramp

LOX and GH2 are injected by a coaxial injector. The major part of the exhaust gas leaves the combustor through the main nozzle (see Fig. 2, centre), a small fraction through the secondary nozzle (SN). This secondary nozzle can be opened and closed continuously by a siren wheel. Thus an acoustic excitation of a well defined frequency can be coupled in the combustion chamber.

The spectrum of the eigenmodes of the combustion chamber can be determined by tuning the excitation frequency with a linear ramp during an experiment (see Fig. 2, right side).

3.3 Measurement Techniques

To visualize the combustion process two high speed CCD cameras were used. With a Photron Ultima 1024 C (16000 *frames/s*, resolution 256x32 *pixel*) the spray was observed and with a Photron Ultima I2 (27000 *frames/s*, resolution 128x64 *pixel*) the flame emission was detected. Additionally a photomultiplier was used to measure locally the intensity of the flame emission. Both photomultiplier and high speed camera were equipped with an interference filter with a transmission at the wavelength of the OH-chemiluminescence near 307 *nm*. Fig. 3 shows the optical set up.
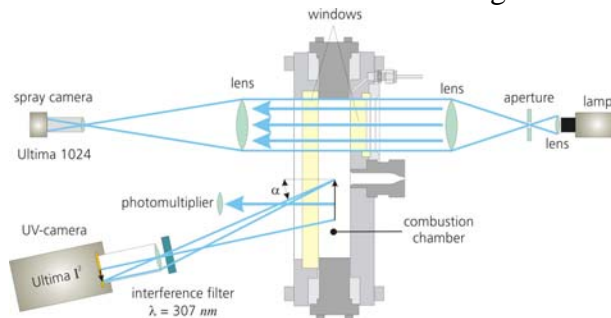

Fig. 3: High speed video visualization

The data acquisition rate of static pressure and temperatures as well as mass flows was $1kHz$, the dynamic pressure sensors and the speed of the siren wheel (measured with a photo diode) were sampled with $27kHz$. This sampling rate was chosen to be able to compare the pressure data with the heat release data measured by the high speed video camera with the same frame rate.

3.4 Test Performance and Variation of Parameters

The LOX/GH2 spray is ignited by a pilot flame. After around four seconds the combustion is nearly stable at constant combustion chamber pressure and constant mixture ratio. At four seconds the siren wheel starts to accelerate with a linear ramp of $400Hz/s$. At around six seconds the resonance frequency of the first tangential mode is reached. Shortly before both high speed cameras were triggered to start their image acquisition. After 10 seconds a test is finished because of the thermal load of the combustion chamber. The parameters that were varied are (a) the position of the secondary nozzle from 0° to 180° relative to the injector axis to fix the nodes and anti nodes, (b) different injectors to check the influence of the geometry and the injection conditions like velocity ratio, Weber number or momentum flux, (c) different main nozzle diameters to vary the combustion chamber pressure between $1.1bar$ and $10bar$. By adjusting the tank pressures and using orifices in the feed lines a mixture ratio range between 2 and 9 (equivalence ratio 0.9 … 4) could be realized.

3.5 Data Analysis

Analysis of pressure: A spectrogram of the dynamic pressure between ignition and shut down shows the increase of the excitation frequency according to the ramping of the siren wheel and the frequency of the modes. Whenever the excitation frequency corresponds to an eigenfrequency of the combustor the dynamic pressure amplitude is increased. The peak-to-peak value p' of the dynamic pressure p on resonance is taken to quantify the pressure response p'/p. In special cases a band pass filter was applied to the pressure data. Then the maximum pressure fluctuation of each dynamic sensor was used to recalculate an averaged 2D pressure field which can be compared with the numerically calculated pressure field of a cylindrical volume coupled to a resonator.

OH-image analysis: Each image of the image sequence recorded with the high speed CCD camera is analyzed locally on squares or stripes (Fig. 4). In each area of interest a spatial mean grey value I is calculated. From the image sequence thus the spatially resolved evolution of the OH-intensity $I(t)$ can be determined. $I(t)$ contains the variation of the flame intensity in the frequency range of the excitation frequency $I(t)=I+I'\cdot cos(\omega t+\varphi)$. The amplitude of the flame response I' in this frequency range is determined with a similar procedure as in the case of the dynamic pressure. The value I'/I thus characterizes the flame response due to the external excitation.
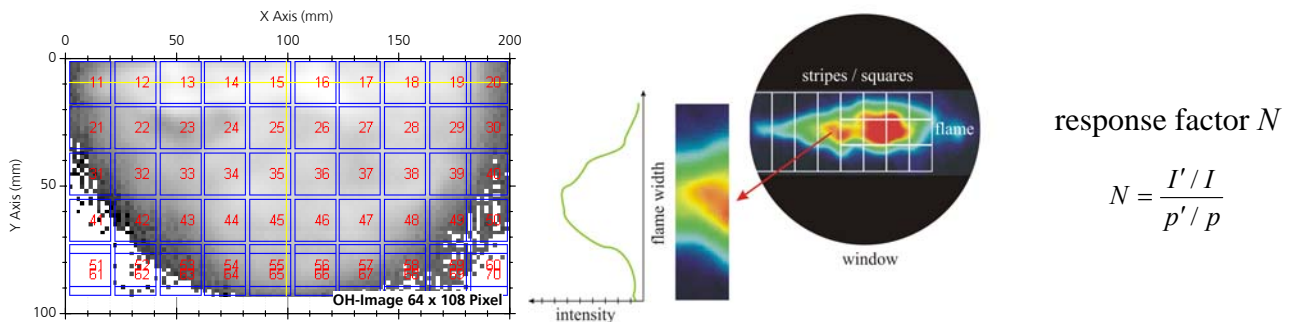

response factor N

$$N = \frac{I'/I}{p'/p}$$

Fig. 4: Analysis window divided in squares or stripes

4 RESULTS

Fig. 5 shows on the left side an example of *p(t)* and its spectrogram and on the right side the FFT spectrum of *p(t)* for *t* = 4 … 9 seconds. As clearly can be seen in the spectrogram the siren starts with a frequency of 3*kHz* and after three seconds – at this time the combustion is nearly stable – the wheel is accelerated with 400*Hz/s*. After nine seconds the frequency of 5.4*kHz* is reached, and after further 0.5*s* the siren was slowed down to 100*Hz*. Because the excitation of the siren is not harmonic the second harmonic of the siren wheel with starting at 6*kHz* can also be seen in the spectrogram.
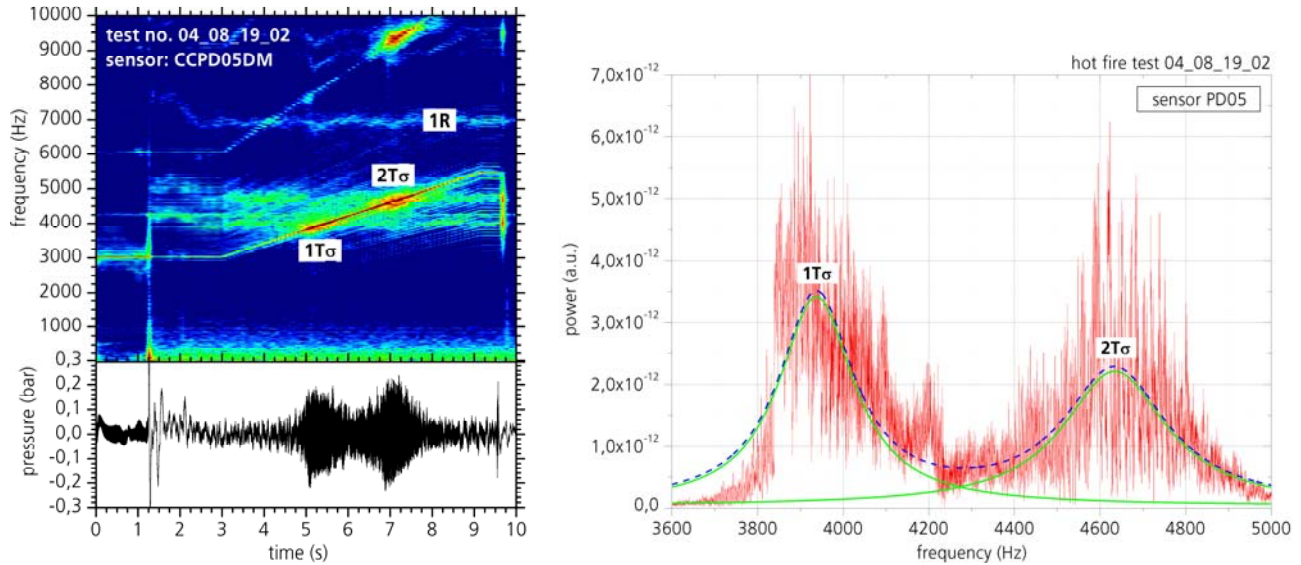

Fig. 5: 1Tσ and 2Tσ resonances in hot fire test

In the spectrogram the eigenfrequencies of the transverse modes 1T, 2T, and 1R can be seen. Whenever the excitation frequency of the siren wheel matches an eigenfrequency the dynamic pressure amplitude increases. With these resonance frequencies the speed of sound and the temperature in the combustion chamber can be recalculated. In the present test a speed of sound of app. 1400*m/s* could be determined.

The frequency distribution on the right side of Fig. 5 shows a maximum of the 1Tσ mode at around 3950*Hz* and the 2Tσ mode near 4650*Hz*. Lorentzian line shapes are fitted to the resonance profiles. It is clearly seen, that the resonance profile is very strongly structured and not a pure Lorentzian. The reason for the complex line profile is not resolved up to now.

As surely noticed in Fig. 5 the two resonances 1T and 2T at the time app. 5*s* and 7*s* are lying close together. This is a result of the secondary nozzle as can be explained by Fig. 6.

In this figure the left graph in the left half shows the frequency spectrogram of a combustion chamber without additional resonator. The modes from below to above are in this order 1T, 2T, 1R, 3T and 4T. In the right half a test with secondary nozzle can be seen. The virtual splitting of the 1T mode in 1Tσ and 2Tσ as a result of the cavity (see section 2.3) is obvious (see arrow). The sharp frequency at 4.3*kHz* is an artefact of the pressure sensor.

It also can be seen in Fig. 6 (right side) that with increasing length of the cavity the eigenfrequency of the σ-component is changing while the frequency of the π-component remains nearly constant. In the experiments no excitation of the π-mode is possible because of the excitation geometry, so only the two related resonances 1Tσ and 2Tσ can be observed.
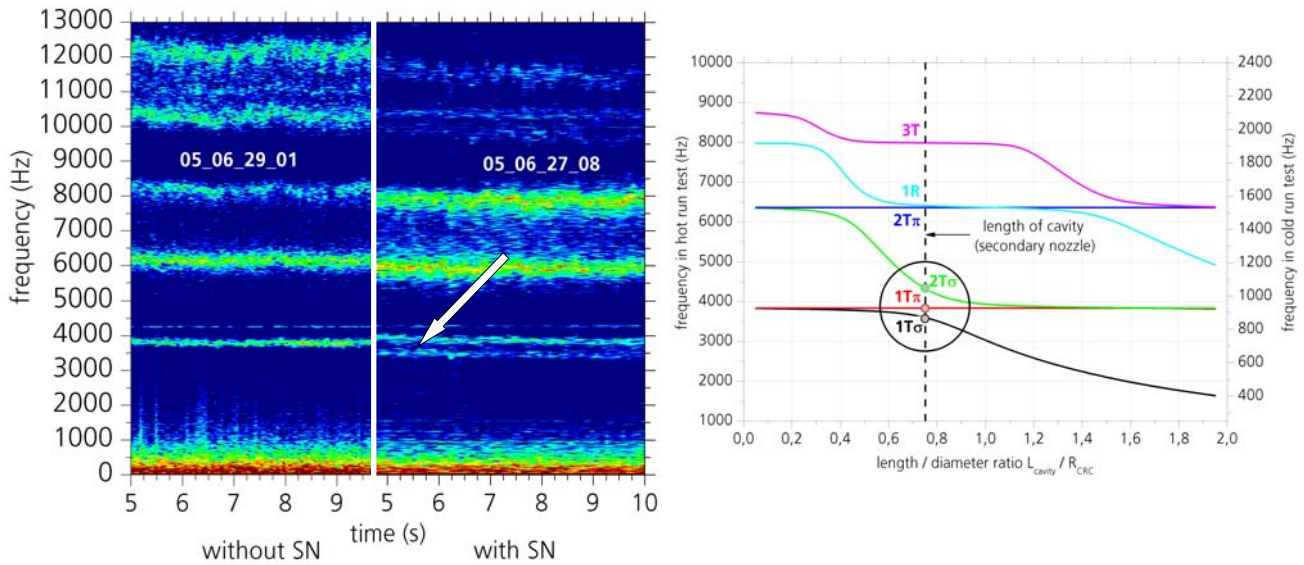
Fig. 6: Influence of an additional resonator (SN = secondary nozzle)

If the combustion is excited by the secondary nozzle the orientation of the mode is adjusted by the position of the secondary nozzle as can be seen in Fig. 7.
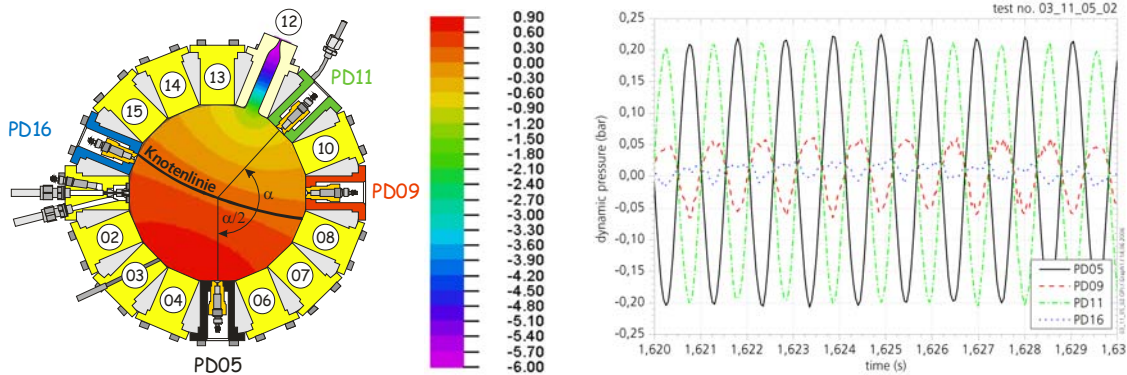

Fig. 7: Orientation of pressure nodal line adjusted by secondary nozzle

Fig. 7 shows the pressure signal for an interval of 10 milliseconds. During 1Tσ resonance sensor PD05 and sensor PD11 have about the same amplitude and are exactly 180° phase shifted, that means the pressure nodal line is positioned between both. Sensor pairs PD09/PD11 and PD16/PD05 show the same phase and consequently each pair have to be positioned at the same side of the nodal lines. Because of the lower amplitude of sensors PD09 and PD16 in comparison to sensors PD05 and PD11, the position of sensors PD09 and PD16 must be closer to the nodal line than the others. Thus from the amplitudes and the phases the orientation of the 1Tσ mode as shown in Fig. 7 can be reconstructed.

Fig. 8 shows that the signals of the photomultiplier, the high speed camera, and the signal of sensor PD05 have a phase difference of $\varphi = 0°$. All these sensors are positioned at the same side of the nodal line. Thus flame emission (heat release) and dynamic pressure are in phase, the Rayleigh criterion is positive: The coupling of the acoustics to combustion results in an energy transfer from combustion to acoustics.
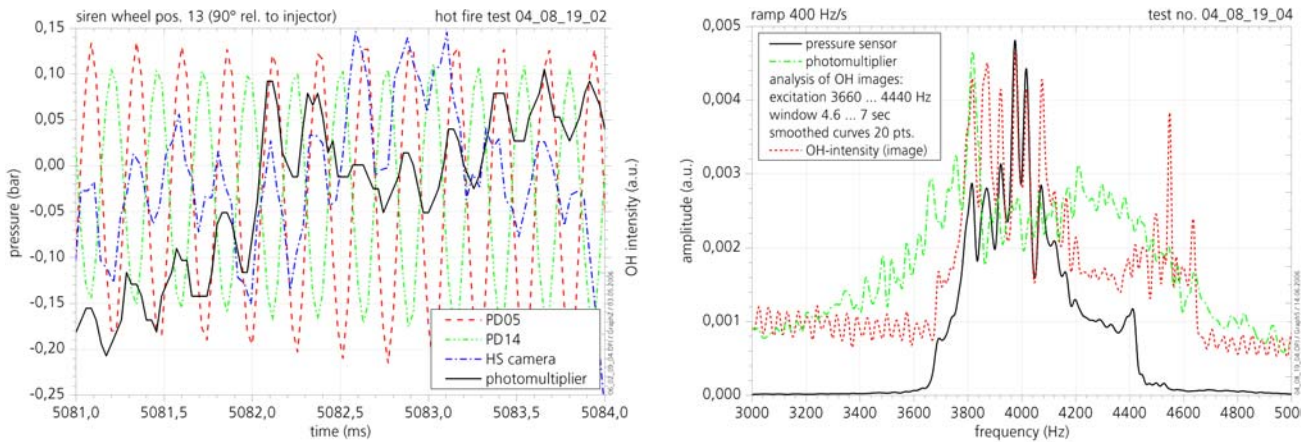
Fig. 8: Left: Phase relation between of pressure and intensity, Right: Frequency spectra

In the right graph of Fig. 8 the 1Tσ resonance spectra of pressure and OH-intensity (OH images and photomultiplier) are shown. OH image acquisition was active when the excitation frequency was ramped between $3660Hz$ and $4440Hz$. A good agreement of the spectral signature of pressure and intensity (heat release) data can be observed. Thus the non-Lorentzian, complex spectral signature on resonance is confirmed by two physical properties, pressure and heat release.

In Fig. 9 a sketch of the experimental configuration and the 1T-mode orientation is shown for a siren wheel position of 90°. The spray is injected from left to right. Due to the limited size of the window the full length of the spray is not known.
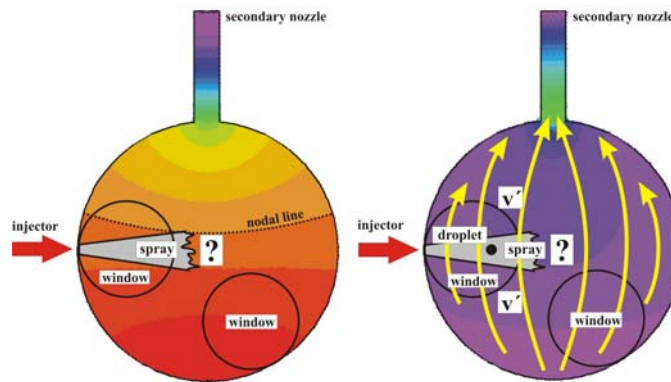

Fig. 9: Left side: pressure distribution; right side: velocity distribution

The velocity field is perpendicular to the pressure nodal line. The spray axis is parallel and near to the pressure nodal line. That means that there is a small interaction of pressure fluctuations with the spray. A LOX droplet in the spray is thus experiencing high acoustic velocity fluctuations and only low pressure fluctuations. The sign of the acoustic velocity changes during one period of oscillation. However because the velocity of the droplet and the acoustic velocity are perpendicular the interaction should be independent of the sign.

If only the magnitude of the velocity is considered the left graph of Fig. 10 shows that the velocity oscillates with the double frequency (2ω) compared with the pressure. In the case of a velocity coupling heat release should also oscillate with twice the frequency of the pressure. Looking to the frequency spectrum of the mean intensity measured in the whole small window it can be seen that there is no resonance at $2\omega = 7800Hz$ (see Fig. 10, circle).
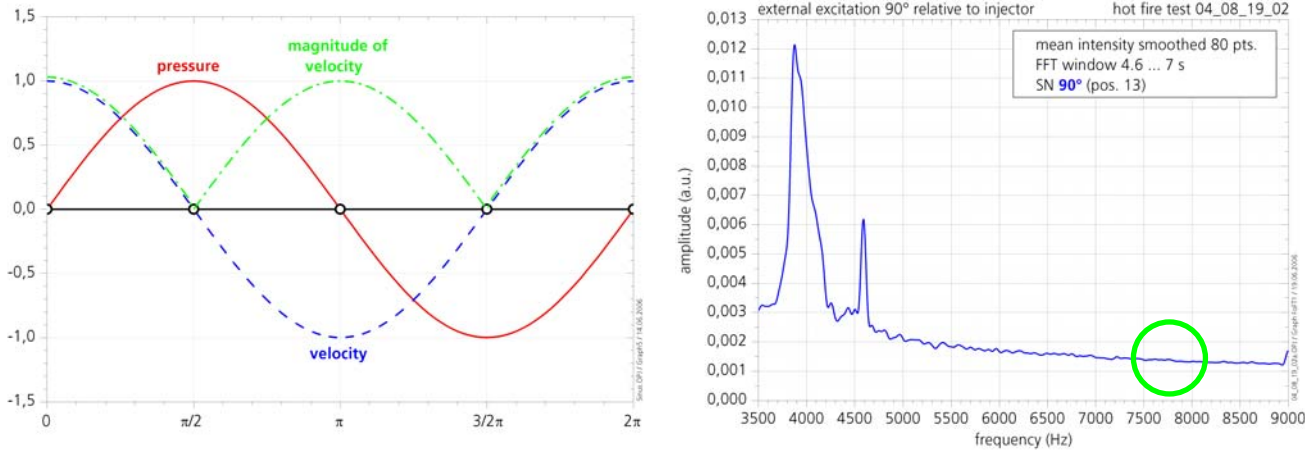
Fig. 10: Right side: phase information of pressure and velocity; left side: frequency distribution of OH intensity

The high amplitude at $3900 Hz$ belongs to the resonance frequency of the $1T\sigma$ mode while the peak at $4600 Hz$ to the $2T\sigma$ mode. That means that at 1T resonance there is no velocity coupling with heat release. The spray experiences only a pressure coupling.

In the following the 2D distributions of the flame intensity and pressure fluctuations are discussed (see. Fig. 11). The graphs in Fig. 11 map the lower half of the combustion chamber.

(a) mean OH intensity I_{mean}

(b) intensity fluctuation I'

(c) relative intensity fluctuation I'/I_{mean}
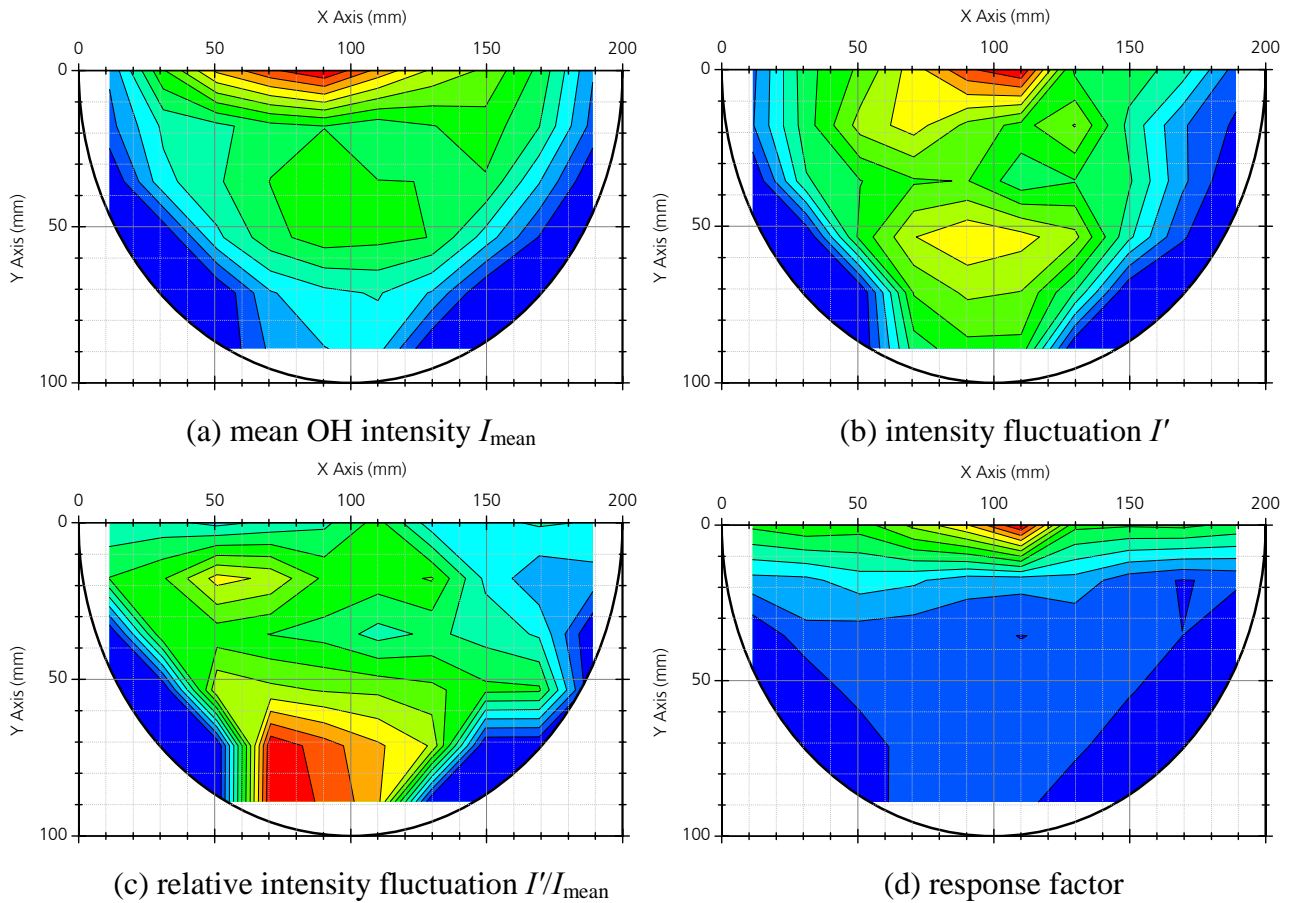

(d) response factor

Fig. 11: Flame response during external excitation 90° relative to injector axis

The injector is positioned at the left side of each graph at position x=0, y=0. The diameter of the combustion chamber is 200*mm*. The chamber was excited in this test with the siren wheel at 90° relative to the injector. As clearly can be seen the mean intensity *I* is the highest at the injector axis and in the centre of the combustion chamber (red colour symbolizes high values and blue colours indicate low values). This just reflects that the flame burns around the LOX/H2-spray. The intensity fluctuation *I'* has also the highest value in the centre of the chamber. In the other part of the combustion chamber, *I'* shows relatively low values. Looking to the relative intensity fluctuation *I'/I* the similarity to the pressure distribution at 1T resonance is obvious. The highest amplitudes were observed at the location of pressure anti-nodes and the lowest fluctuation was measured at the nodal line which is at the injector axis. This is a further indication for a coupling between heat release and acoustic pressure.

The response factor *N = (I'/I)/(p'/p)* shows the main response at the injector axis, that means that the main processes during an instability will take place in the spray region or rather in the vaporization and mixing zone. Just below the injector axis nearly no response can be seen.

5 CONCLUSIONS

The performed tests showed that the orientation of the tangential modes in a combustion chamber can be controlled by the secondary nozzle working as a cavity. The pressure nodal line can be adjusted by the position of this nozzle. By adjusting the pressure field by the secondary nozzle the investigation of the influence of a pressure node or anti node to the different combustion chamber processes is possible.

With the help of the analysis of the OH flame emission it is possible to draw conclusions from the heat release in the flame. During resonance conditions no phase shift could be seen between pressure and intensity fluctuations. According to the Rayleigh criterion thus the coupling of the acoustics to the flame should be positive. The simultaneous spatially resolved measurement of pressure and flame intensity leads to the derivation of the response factor. The main response was observed at the spray axis that means directly in the spray. From the spatial distribution of the relative flame fluctuation it is concluded that during a 1T resonance the acoustics/flame coupling is due the acoustic pressure.

REFERENCES

1. Yang V and Anderson W (Eds.). *Liquid Rocket Combustion Instability*. Progress in Astronautics and Aeronautics, Vol. 169, 1995.
2. Harrje D and Reardon F (Eds.). *Liquid Propellant Rocket Combustion Instability*. NASA SP-194, 1992.
3. Putnam A. *Combustion-Driven Oscillations in Industry*. American Elsevier Publishing Company, Inc., New York, 1971.
4. Heidmann M and Wieber P. *Analysis of Frequency Response Characteristics of propellant Vaporization*. NASA TN D-3749, 1966.